Phospholipid Regulates the Activation of Factor X by Tissue Factor/Factor VIIa (TF/VIIa) via Substrate and Product Interactions

James J. Hathcock,*,† Elena Rusinova,† Rodney D. Gentry,‡ Harry Andree,† and Yale Nemerson†

Department of Medicine, Mount Sinai School of Medicine, Box 1269, One Gustave Levy Place, New York, New York 10029, and Department of Mathematics and Statistics, University of Guelph, Guelph, Ontario, Canada N1G139

Received February 23, 2005; Revised Manuscript Received April 13, 2005

ABSTRACT: Although the phospholipid requirement for tissue factor (TF) activity has been well-established, the mechanism by which the surface regulates enzymatic activity remains unclear. We added phospholipid vesicles to already relipidated TF (30/70 PS/PC) and found that added lipid can both enhance and inhibit the rate of factor X (F.X) activation. Using active-site-inhibited F.Xa we demonstrate that F.Xa is a more potent inhibitor of TF/VIIa at lower lipid concentrations, and that this inhibition is attributable to high surface occupancy by F.Xa near the enzyme. We also find that exactly twice as many F.Xa molecules are bound to a lipid surface at saturation as F.X, and that a dimer model of F.Xa binding to the lipid can account for the experimentally observed, preferential binding of F.Xa (compared to F.X) to phospholipid surfaces. We manipulated the amount of phospholipid available to each TF molecule by controlling vesicle size and the number of TF molecules per vesicle and found that, as the 2D radius of phospholipid available to each TF molecule was increased, the observed k_{cat} increased hyperbolically toward a maximum or "true k_{cat}". At a 2D lipid radius of ∼37 nm, the observed k_{cat} was 50% of the "true k_{cat}". Thus, phospholipid surface serves as a conduit for F.X presentation and F.Xa removal, and the rate at which F.Xa leaves the vicinity of the enzyme, either by lateral diffusion or desorption from the surface, regulates the rate of F.X activation. We argue that these findings require reevaluation of existing models of coagulation.

The ability of acidic phospholipid surfaces to accelerate blood coagulation reactions is unquestionably true, but the precise mechanism for this phenomenon is largely unknown. While it is clear that many coagulation proteins bind tightly to phospholipid surfaces, it is unclear to what extent restricted rotational freedom or increased local "concentration" contributes to these rate enhancements. A reaction that initiates coagulation involves tissue factor (TF)[1], a single membrane-spanning protein, which binds and allosterically activates a serine protease, factor VIIa; this complex then proteolytically activates two serine protease zymogens, factors IX and X. These reactions are frequently studied by inserting TF into phospholipid vesicles, thereby restricting reactions to, or close to, the lipid surface. Notably, these enzymic species each contain a cluster of γ-glutamic acid residues that bind Ca^{2+} and acidic headgroups. Thus, enzyme and substrate are well-oriented with respect to the membranes and to each other.

It has been argued whether free F.X or lipid-bound F.X serves as the functional substrate for TF/VIIa. Our group previously reported evidence supporting the notion that free F.X regulates the reaction velocity. Others later reported that lipid-bound substrate was the functional substrate, irrespective of whether F.X was bound proximate to the enzyme or on a distant "naked" vesicle (*1*). Certainly, lipid-bound F.X is properly oriented with respect to the membrane, favoring productive collisions with TF/VIIa; however, from consideration of diffusion and collision theory, we conclude that lipid-bound F.X far away from the enzyme complex or on a separate lipid vesicle will take much longer to encounter the enzyme and its contribution to product formation is likely small. Although the present study does not directly address the mechanism by which F.X encounters the enzyme, we do contend that F.X is bound to the membrane within a conceptual capture radius (*2*) of the enzyme when it encounters TF/VIIa, and that F.Xa leaves the enzyme laterally via surface diffusion and "hopping". The notion that F.Xa leaves the enzyme onto the adjacent membrane is supported by recent measurements by Erb (*3*) indicating that the off-rate of F.Xa from the membrane is much slower than the k_{cat}. In the present study, we show that the total amount of phospholipid relative to TF, as well as the spatial arrangement of the lipid with respect to TF, both regulate the enzymatic activity of TF/VIIa and that phospholipid can have both an enhancing and inhibitory effect on TF/VIIa activity.

* Corresponding author: James J. Hathcock, Mount Sinai School of Medicine, Box 1269, Department of Medicine, One Gustave Levy Place, New York, NY 10029. Phone: 212 241-6083. Fax: 212 860-7032. E-mail: James.Hathcock@mssm.edu.

† Mount Sinai School of Medicine.

‡ University of Guelph.

[1] Abbreviations: βOG, *n*-octyl-β-D-glucopyranoside; BSA, bovine serum albumin; D_v, vesicle diameter; DOPS, 1,2-dioleoyl-*sn*-glycero-3-phosphatidylserine; DOPC, 1,2-dioleoyl-*sn*-glycero-3-phosphatidylcholine; EDTA, ethylenediamine tetraacetate; F.X, factor X.; F.Xai, active-site-inhibited factor Xa; HBS, HEPES-buffered saline; K_D, dissociation constant; K_m, Michaelis−Menten constant; k_{cat}, catalytic rate constant; K_a, monomeric F.Xa dissociation constant; K_b, dimeric F.Xa dissociation constant; MW, molecular weight; *n*, moles of lipid/moles of protein at saturation; *N*, number of TF molecules per vesicle; PSPC, 30% DOPS/30%DOPC (mole/mole); SDS, sodium dodecyl sulfate; TF, tissue factor.

10.1021/bi050338b CCC: $30.25
Published on Web 05/10/2005

MATERIALS AND METHODS

Reagents. 1,2-Dioleoyl-*sn*-glycero-3-phosphatidylserine (DOPS) and 1,2-dioleoyl-*sn*-glycero-3-phosphatidylcholine (DOPC) were purchased from Avanti Polar Lipids, Inc. (Alabaster, AL). ^{14}C-DOPC and *N*-succinimidyl[2,3-^{3}H] propionate were from Amersham Biosciences (Piscataway, NJ). *n*-Octyl-β-D-glucopyranoside (βOG) was purchased from Calbiochem (La Jolla, CA). Spectrozyme F.Xa was purchased from American Diagnostica Inc. (Greenwich, CT). Recombinant human Tissue Factor (TF), contains residues 1−242 of full-length tissue factor and was a generous gift from Genentech (San Francisco, CA). Tracer quantities of TF were labeled with *N*-succinimidyl[2,3-^{3}H] propionate according to the method of Bolton and Hunter (*4*). The specific activity of ^{3}H-TF was 3.68×10^5 dpm/μg. Factor VIIa was a generous gift from Novo Nordisk (Bagsvaerd, Denmark).

Human F.X was purified according to Miletich (*5*). Factor Xa used in binding and kinetic studies was activated from F.X using Russell's viper venom (Enzyme Research Laboratories, South Bend, IN) and purified as described (*6*). F.Xa used in inhibition studies was purchased from Enzyme Research Laboratories (South Bend, IN). N^{α}-[(Acetylthio)-acetyl]-*D*-Phe-Phe-Arg-CH_2Cl (ATA-FFR-CH_2Cl) was prepared according to Bock (*7*), and incubated with ~20 μM F.Xa at a 5−10-fold molar excess for 2 h to inhibit F.Xa (*7*). Excess inhibitor was removed by extensive dialysis against 10 mM HEPES and 0.14 M NaCl, pH 7.4 (HBS), and inhibition of the F.Xa was verified using Spectrozyme-F.Xa.

Reconstitution of TF into Phospholipid Vesicles. TF was incorporated into PSPC (PS/PC 30:70) vesicles using a slow dialysis method. Briefly, phospholipid mixtures containing tracer amounts of ^{14}C-PC were dried under nitrogen. The phospholipids were then solubilized with 150 mM βOG in 0.01 M HEPES, 0.14 M NaCl, and 1 mM NaN_3, pH 7.4. TF and tracer quantities of ^{3}H-TF were added to achieve the desired ratio of TF/PL, and the resulting mixture was dialyzed against HBS containing 20 mM βOG (close to the CMC of βOG (*8*)). A peristaltic pump was employed to remove and replenish dialysate at a slow, constant rate (~1 mL/min) for 72−96 h. Unilamellar vesicles were obtained by extrusion using the Avanti Mini Extruder (Alabaster, AL). The final concentrations of PSPC and TF were determined using a Wallac 1409 counter from Perkin-Elmer (Boston, MA). The slow dialysis method yields TF densities up to 490 fmol/cm^2, which is considerably higher than the densities obtained by typical dialysis. In one set of experiments, we created PSPC vesicles that were 100 nm in diameter and contained various TF densities. In a second set of experiments, the vesicle diameter varied from 10 to 400 nm while keeping an average of 1 exposed TF molecule per vesicle.

Binding of F.X and F.Xa to PSPC Surfaces. The adsorption of F.X and F.Xa to phospholipid bilayers was studied with computer-assisted ellipsometry using methods similar to those previously published (*9*−*11*). Planar PSPC bilayers were generated on silicon slides from vesicles according to previously published methods (*11*−*13*). A 5 mM PSPC vesicle mixture was prepared as described above, except without TF, and extruded through 10−400 nm-diameter (pore-size) membranes. Hydrophobic silicon slides (1 cm × 4 cm × 0.04 cm), cut from silicon wafers (Wacker Chemie, Munich, Germany, n-type, phosphor-doped), were cleaned thoroughly with detergent (Sparkleen, Fisher Scientific) and water and then stored overnight in 30% chromic sulfuric acid. Slides were then flushed with water and stored in 50% alcohol−water until use. At the time of the experiment, slides were washed with distilled water and then placed in a stirred cuvette containing binding buffer (10 mM HEPES, 0.14 M NaCl, and 5 mM $CaCl_2$, pH 7.4). The PSPC vesicle suspension was then added (50 μM final concentration) and continuously stirred for 10 min, during which time the adsorption of the PSPC onto the slide was monitored. The mass of the PSPC bilayer (approximately 0.36 μg/cm^2) was subtracted from the protein adsorption curves. The slide was then washed in binding buffer containing 0.1% BSA. F.X or F.Xa were then added, and the increase in the mass of bound protein was observed (all at 37 °C). Basically, the ellipsometer measures binding to reflective surfaces by monitoring changes in the polarization of the reflected light. The indicated mass of protein per unit area was converted into moles per unit area using the nonglycosylated MWs of F.X and F.Xa, respectively (*9*). The amount of bound protein was plotted as a function of free protein and fit to a hyperbola to obtain the dissociation constant and maximum binding per unit area. The bound versus free protein data were also fit to a sequential dimer model for F.Xa binding, which is described in detail in Appendix A.

To determine if F.X or F.Xa bind competitively to the PSPC surface, a glass tube was cleaned, coated with a PSPC bilayer, and rinsed with buffer with 0.1%BSA as described above. A glass tube was substituted for the silicon slide as it had a larger surface area (11.7 cm^2; functional volume = 1.9 mL). F.X (600 nM) and F.Xa (600 nM) were then added to the tube and incubated for 1 h at 37 °C with constant mixing. Afterward, the volume in the tube was rapidly displaced by more than 50 vol of binding buffer and the bound protein eluted with 1.9 mL of 20 mM EDTA. The eluted protein was electrophoresed on a 0.1% SDS−12% polyacrylamide gel and assayed by standard immunoblot with a mouse anti-human F.X antibody (Accurate Chemical, Westbury, NY) that recognized F.X and F.Xa with equal affinity.

Numerical simulations of the competition of F.X and F.Xa for a fixed phospholipid surface area were performed using both monomeric and dimeric models of F.Xa binding (see Appendix A). In the monomeric model, both proteins compete for lipid surface area where the area occupied by each protein was determined from saturation measurements using ellipsometry. In the dimer model, both proteins compete for a fixed number of lipid binding sites, but a second F.Xa can bind to the first. The equations are outlined in Appendix B and were solved computationally using a FORTRAN implementation of the Livermore Laboratory's ordinary differential equation solver (LSODE).

Initial Rate Kinetic Assays. All kinetic assays were performed using an automated robotic pipetting system (Tecan AG, Switzerland) with internally developed software (*14*). All reagents were preincubated at 37 °C. A TF−vesicle suspension (typically 8 pM TF final concentration) was added to a 1.5 mL Eppendorf tube containing appropriate dilutions of F.X in HBS with 0.1%BSA. This was followed by addition of F.VIIa (100 pM) and inhibited factor Xa (Xai)

where indicated, and the reaction was initiated with 5 mM $CaCl_2$ (all final concentrations; all at 37 °C). Aliquots were removed at timed intervals and placed into wells of a microtiter plate containing 125 μL of 50 mM EDTA, 50 mM bicine, and 0.1% BSA (pH 8.5) to quench the reaction. A chromogenic substrate for F.Xa (Spectrozyme-Xa, 300 μM final concentration) was added to each well, and the initial increase in absorbance at 405 nm was measured using a VERSAMax microplate reader (Molecular Devices, Sunnyvale, CA). Initial slopes of substrate hydrolysis were compared to standard curves obtained with known concentrations of F.Xa to determine the actual concentration of F.Xa at each time point. Standard curves of F.Xa concentration versus the rate of substrate hydrolysis were performed with purified F.Xa under conditions similar to those used experimentally, both with and without PSPC (0−200 μM).

The initial rate of F.X activation for each reaction was determined from a linear, least-squares regression of F.Xa concentration versus time, typically spanning 6 data points over the initial 2−3 min of the reaction. The total percentage of F.X hydrolysis was kept under 10% and was only appreciable when using low starting concentrations of F.X. The kinetic parameters K_m and V_{max} were determined by measuring the initial rate of F.X activation using a range of different starting substrate (F.X) concentrations (2−600 nM) and globally fitting the substrate versus initial rate data to a hyperbola. The apparent catalytic rate constant was calculated as the quotient of V_{max} and the functional enzyme concentration, assuming that 50% of the total TF molecules were facing outward from the vesicle surface and hence functional (*14*).

Lipid Titration. The conditions for the lipid titration experiments were similar to those for the steady-state kinetic assays. The components of the reaction mixture were added to 1.5 mL Eppendorf tubes containing appropriate dilutions of PSPC vesicles. The order of addition and final concentrations of the reagents were 30 pM TF (total), 2 nM F.VIIa, 200 nM F.X, and 5 mM $CaCl_2$.

RESULTS

Phospholipid Titrations. To investigate the effect of added lipid on TF activity, we took lipidated TF preparations containing approximately 64 TF molecules per 100 nm-diameter vesicle and increased the ratio of PSPC/TF by adding "naked" 100 nm-diameter vesicles that contained no TF. The initial reaction velocity was quantified using 200 nM F.X, 2 nM F.VIIa, and 5 mM $CaCl_2$. When naked vesicles are added, there is a small (~22%) but highly reproducible increase in the reaction velocity in the range of 0.04−12 μM PSPC (Figure 1, inset). This small, but unexplained, increase in the reaction velocity is consistent with the view expressed by Krishnaswamy (*1*) that all lipid, regardless of whether it is on a vesicle associated with TF or on a naked vesicle lacking TF, serves to make the zymogen a better substrate for the extrinsic Xase complex. However, further addition of PSPC (containing no TF) decreased the reaction velocity (Figure 1); at 400 μM PSPC, the velocity was only 10% of the maximum observed. This observation is inconsistent with the previous view and suggests that naked lipid serves to partition F.X far away from the enzyme complex. Thus, in the present experiments,

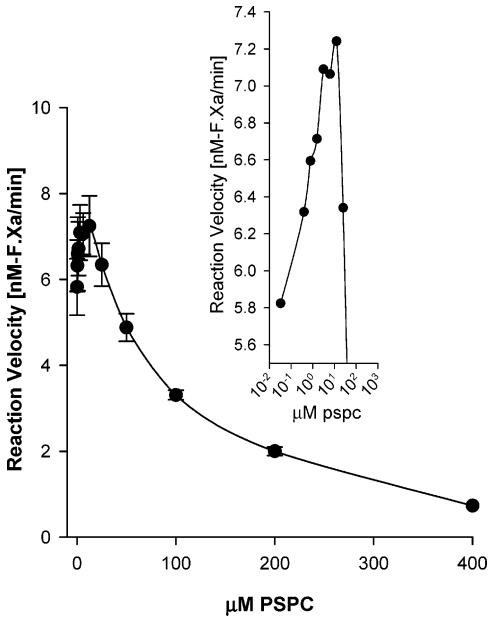

FIGURE 1: Various concentrations of 100 nm-diameter PSPC vesicles devoid of TF were added (abscissa) to a preparation of already lipidated TF (30 pM TF and 40 nM PSPC), and the initial rates of F.X activation were measured (200 nM F.X, 2nM F.VIIa, and 5 mM $CaCl_2$). Thus "naked" lipid can have both enhancing and inhibitory effects on F.X activation.

naked lipid vesicles served to both increase and decrease the reaction velocity depending on the quantity added.

Binding of F.X and F.Xa to PSPC Surfaces. To understand the extent to which F.X and F.Xa binding to PSPC could influence our experiments, we measured their binding parameters using ellipsometry, a true equilibrium technique. The data in Figure 2 show separate binding isotherms for F.X and Xa, each derived from three separate experiments. The data points were fit globally to classic binding isotherms for monolayer binding. The K_D for F.X binding to the lipid bilayer was 34.2 ± 2.9 nM, and binding approached a saturation density of 4.2 ± 0.1 pmole-F.X/cm^2 (Γ_{max}; r^2_{adj} = 0.97). The K_D for F.Xa binding to the bilayer was 53.9 ± 2.6 nM, and binding approached a saturation density of 8.5 ± 0.1 pmole-F.Xa/cm^2 (Γ_{max}; r^2_{adj} = 0.99). The molar ratios of phospholipid to protein at saturation (*n*) were 106 for F.X and 52.1 for F.Xa.

Interestingly, the maximum binding capacity for F.Xa was twice that observed for F.X. On the basis of the intact F.X structure (*15*), we calculated the largest 2D cross-sectional area of F.X parallel to the membrane (23.2 nm^2) and estimated the maximum density of F.X molecules that could be packed side-by-side on the membrane (7.1 pmol/cm^2). Our experimental measurements thus correspond to a 59% efficient use of the 2D space for F.X. The β-form of F.Xa (undergoes two separate cleavages) has a smaller maximum cross-sectional area (16.8 nm^2) than F.X, and we estimate the maximum possible monomeric surface density to be 9.9 pmole/cm^2. This corresponds to an 86% efficient use of the 2D space, which is very high; the maximum packing efficiency of highly organized, hexagonally packed cylinders is 91%, and they are not surrounded by an electrorepulsive static field. Thus, whereas it is theoretically possible to pack 8.5 pmole-F.Xa/cm^2 side-by-side on a surface, it would require an exceptionally high degree of organization and a 46% better use of space than for F.X. Furthermore, reports

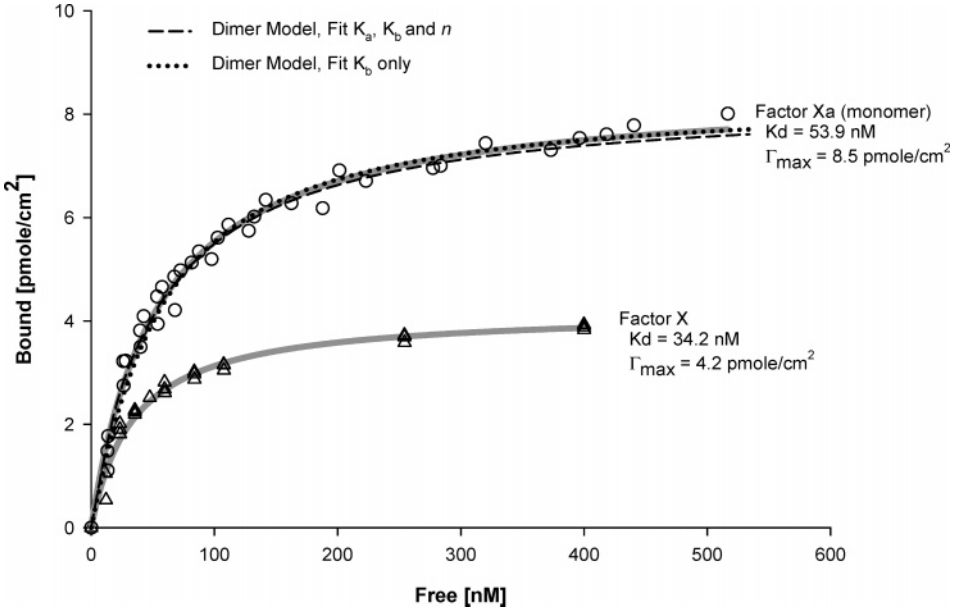

FIGURE 2: The binding of F.X (△) and F.Xa (○) to a PSPC bilayer was measured by ellipsometry and fit to classic, hyperbolic binding isotherms (solid gray lines). The F.Xa data were also fit to a dimer binding model (− − −), and to a dimer binding model under the assumption that F.X and F.Xa both have identical lipid-binding characteristics and differ solely by virtue of the ability of F.Xa to form a dimer (...).

by Majumder using semisoluble 6CPS (*15*), have suggested that F.Xa dimerizes when interacting with PS in the presence of Ca^{2+}.

We thus entertain the notion of F.Xa dimerization on the lipid surface, by constructing the following sequential dimer model for F.Xa binding to PSPC, where L represents a lipid binding site, P (product) is free F.Xa, LP is lipid-bound F.Xa, and LD is lipid-bound dimeric F.Xa. K_a and K_b are the respective dissociation constants as shown.

$$P + L \underset{K_a}{\longleftrightarrow} LP$$

$$P + LP \underset{K_b}{\longleftrightarrow} LD$$

For simplicity, we have neglected the possibility that the F.Xa dimer may directly dissociate into two separate bound Xa monomers, favoring an approach that resembles the more classical case of ligand binding. The relationship between bound, free, and total Xa at equilibrium simplifies to a cubic equation with one physically realistic solution (see Appendix A). We fit the same data obtained from equilibrium binding experiments to the sequential dimer model and obtained $K_a = 26.1 \pm 2.7$ nM, $K_b = 104 \pm 19.6$, and $n = 106.2 \pm 2.9$ mol of phospholipid/moles of protein at saturation ($r^2_{adj} = 0.98$). If we assume that a F.Xa monomer and F.X both interact identically with the PSPC surface ($n = 106$ and $K_{D,F.X-L} = K_a = 34.2$ nM) and that F.Xa differs only by virtue of being able to form a dimer on the surface, then the best fit for the dimer dissociation constant, K_b is 88.2 ± 18.6 nM, whereupon $K_a = 34.2 \pm 4.4$ nM and $n = 106 \pm 2.0$ ($r^2_{adj} = 0.98$). Graphs of these two-dimer model fits are shown in Figure 2, and both match the data extremely well. Hence, it is unlikely that typical equilibrium binding measurements could discriminate decisively between the true nature of either monomeric or dimeric binding. Furthermore, F.X and F.Xa may be identical in their binding to PSPC, and only differ by the ability of F.Xa to form the dimer.

Dimer versus Monomer F.Xa Models: Validation of F.Xa Dimer Model. Once the binding parameters of F.X and F.Xa were established, we conducted numerical simulations of the competitive binding of F.X and Xa to PSPC using both a monomeric and dimeric model for F.Xa (see Appendix B). In the monomeric F.Xa model, F.Xa occupies half the lipid area as F.X does, and both compete for lipid surface area. In the dimer F.Xa model ($K_b = 88.2$ nM; $K_a = 34.2$ nM, and $n = 106$), F.X and F.Xa compete equally for identical PSPC-binding sites, but differ by virtue that a second F.Xa can bind to a lipid-bound F.Xa. In the monomeric F.Xa model, when large equimolar concentrations of F.X and F.Xa compete for a limited PSPC area, 56% of the protein bound to the surface is F.Xa and 44% is F.X. In contrast, the dimeric F.Xa model predicts that under the same conditions the surface will be occupied almost entirely by F.Xa. To test these models experimentally, we performed a lipid-binding assay similar to those with the ellipsometer in which a glass tube (instead of a planar silicon chip) was coated with a phospholipid bilayer and incubated with 600 nM F.X and 600 nM F.Xa for 1 h with stirring. Afterward, the protein solution was displaced and the lipid surface washed with >50 tube volumes of buffer (5 mM $CaCl_2$ and 0.1% BSA in HBS). The bound protein was eluted from the lipid surface with EDTA and assayed for F.X and Xa content by Western blot (a semiquantitative technique) using a monoclonal detection antibody that equally recognized the nonreduced forms of F.X and F.Xa. According to the dimer model simulation, 93% of the bound protein will be F.Xa and 7% F.X; according to the monomeric F.Xa model simulation, 56% of the bound protein will be F.Xa and 44% F.X. Figure 3 shows that over 90% of the signal detected on the blot was attributable to F.Xa, indicating the dimer model more accurately describes the binding of F.X and Xa to PSPC. A sample of the bulk phase F.X and F.Xa mixture following the incubation is also shown. In a subsequent experiment, we incubated only F.X (600 nM) with the lipid-

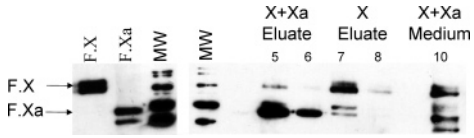

FIGURE 3: Western blot showing the preferential binding of F.Xa over F.X to a PSPC surface. A solution of 600 nM F.X and 600 nM F.Xa was incubated in a PSPC-coated tube (equivalent to 2.7 μmol/L PSPC); the bound protein was eluted with EDTA and assayed by western blot using an antibody that recognized F.X and F.Xa equally. Lanes: (1) F.X, (2) F.Xa, (3 and 4) MW, (5 and 6) 30 and 6 μL of eluate from surface incubated with 600 nM F.X + 600 nM F.Xa, (7 and 8) 30 and 6 μL of eluate from a surface incubated with 600 nM F.X only, and (10) the supernatant containing 600 nM F.X and F.Xa after 1 h incubation with the surface.

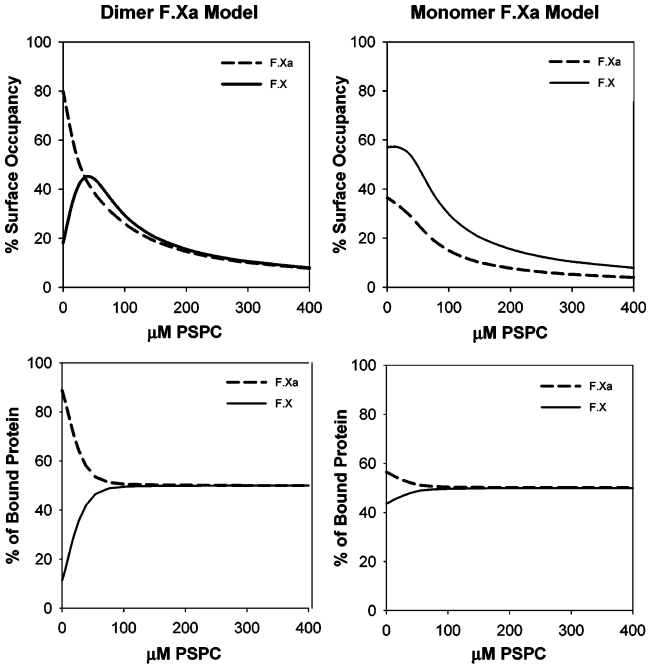

FIGURE 4: Simulations of the competitive binding of F.X (substrate, 300 nM) and F.Xa (product, 300 nM) to PSPC using (left) a dimer F.Xa model in which both proteins compete for an identical number of lipid-binding sites or (right) a monomer model in which both proteins compete for available PSPC surface area. Upper graphs show the percentages of the total lipid surface area occupied by substrate or product, and the lower graphs show the percentage of bound protein attributable to substrate or product. In the dimer model there is an intermediate PSPC concentration yielding a maximum surface density of F.X.

coated surface and eluted it in the same manner, demonstrating that, in the absence of F.Xa, F.X will bind, elute, and be detected in our system. These results clearly show that under limited PSPC conditions F.Xa binds preferentially and that under high, equimolar bulk concentrations of F.X and F.Xa the surface is occupied almost entirely by F.Xa.

Implications of the F.Xa Dimer Model. In accordance with the dimer model simulations, at low-lipid concentrations, F.Xa is preferentially bound to the lipid surface, thereby diminishing the surface density of F.X. Figure 4 shows the percentage of total protein bound attributable to F.X and F.Xa as a function of PSPC concentration for both monomeric and dimeric F.Xa models, given initial concentrations of 300 nM free F.X and 300 nM free F.Xa. This illustrates the concept validated above in which F.Xa binds preferentially to the surface in a dimer model, but almost equally in a

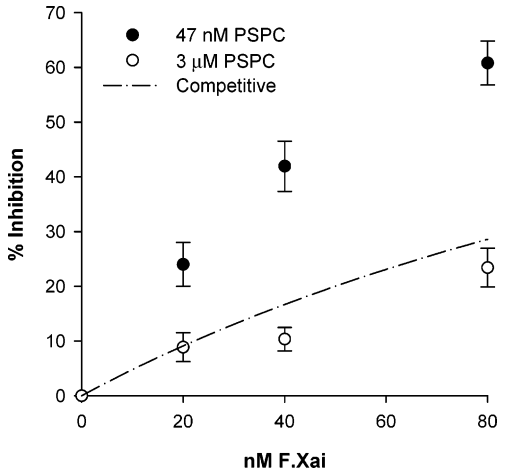

FIGURE 5: F.Xai is a more potent inhibitor at lower lipid concentrations. Inhibition of F.X activation by F.Xai was measured using TF preparations made with either a low-lipid concentration (30 pM TF and 47 nM PSPC) or an intermediate-lipid concentration (30 pM TF and 3 μM PSPC; all 200 nM F.X). The line represents the expected level of inhibition if F.X and F.Xa compete identically for binding to the enzyme complex.

monomer model. Figure 4 also shows the percentage of the lipid surface area occupied by F.X or F.Xa as a function of PSPC concentration. As the lipid concentration is increased, the percentage of the area occupied by F.Xa diminishes rapidly and the surface density of F.X increases through a maximum. This maximum shifts to the left or right with different concentrations of F.X and F.Xa. At high concentrations of PSPC, the surface densities of both F.X and F.Xa decrease almost proportionally with increasing PSPC. If the surface density of F.X mediates TF/VIIa activity, then in the presence of F.Xa, there is a particular intermediate concentration of PSPC yielding a maximum reaction rate, which, using our experimental conditions, occurs at ~12 μM total lipid.

Inhibition by F.Xai. Active site-inhibited F.Xa (F.Xai) is thought to be a competitive inhibitor of TF/VIIa by virtue of its ability to bind to the enzyme complex in place of F.X. If F.Xa and, consequently, F.Xai bind preferentially to PSPC as suggested by the dimer model, then the resulting high surface occupancy of F.Xai at low-PSPC conditions would likely increase the potency of the inhibitor. To test this hypothesis, we prepared TF-vesicles containing 47 nM or 3 μM PSPC (30 pM TF, prepared by detergent dialysis) and assayed the initial rate of F.Xa generation in the presence of 2 nM F.VIIa, 5 mM $CaCl_2$, 200 nM F.X, and varying doses of the inhibitor, Xai (0−80 nM; all final concentrations). Figure 5 shows the percent inhibition of each preparation as a function of F.Xai concentration. As expected, the inhibition by Xai was dose-dependent. However, the inhibitor was decisively more potent on the preparation containing only 47 nM PSPC as compared to the preparation containing 3 μM PSPC. Thus, the lipid content clearly has a nonclassical effect on the inhibition of TF/VIIa by Xai. The line in Figure 5 indicates the theoretical level of inhibition if Xai acted solely as a competitive inhibitor, with binding characteristics to the enzyme identical to those of F.X; that is, F.Xai acts as a nonproductive F.X molecule.

To determine if surface crowding or preferential binding of F.Xai to PSPC could explain the enhanced potency of Xai, we added naked PSPC vesicles to the 47 nM PSPC

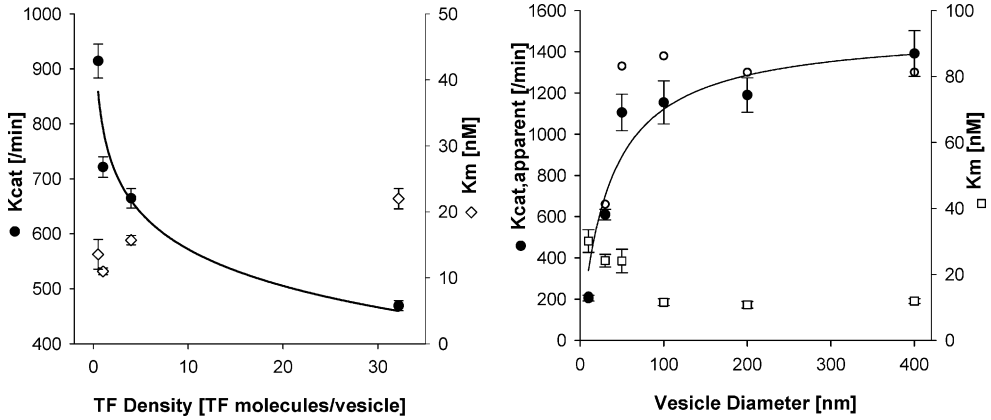

FIGURE 6: The experimentally observed "constants", k_{cat} and K_m, change as a function of (left) the number of TF molecules per 100 nm-diameter vesicle or (right) as a function of the size of the vesicle while keeping one TF per vesicle. The open circles on the right represent k_{cat} values determined from experiments in which naked vesicles were added to maintain a constant overall lipid concentration (3 μM PSPC); the open circle for the lowest PSPC concentration overlaps the filled circle. Thus the spatial orientation of lipid with respect to TF regulates the observed kinetic parameters.

preparation such that the final PSPC concentration was 3 μM. For the case of 80 nM F.Xai, the percent inhibition dropped from 60% to 20% upon the addition of naked vesicles, which was similar to the level observed with the 3 μM PSPC preparation created by dialysis. Similar experiments using up to 80 nM noninhibited F.Xa yielded near-identical results (data not shown). Consequently, lower lipid concentrations enhanced the potency of Xai, and higher concentrations of PSPC, whether on the same vesicle as TF or on naked vesicles, served to relieve the inhibition, presumably by diluting the surface density of Xai.

Effect of PSPC on K_M and k_{cat}. In the above studies, we primarily considered cases in which F.X, Xa, and Xai were each distributed uniformly among the available phospholipid surface. In the case of a reaction where F.Xa is generated at the site of the enzyme, there will be a temporal accumulation of Xa near the enzyme. At steady state, the rate of accumulation will be balanced by the rate of Xa generation and the rates at which it diffuses laterally away from the enzyme, the rate at which it leaves the lipid surface, and the rate at which it diffuses away from the active vesicle possibly to a naked vesicle. Therefore, because of its proximity to the enzyme, F.Xa generated at the site of the enzyme will likely be more potent than an equivalent amount of Xa (or Xai) distributed uniformly throughout the milieu. To investigate the effect of the spatial localization of PSPC relative to TF on the reaction kinetics, we manipulated the TF and PSPC in one of several ways: (i) using 100 nm-diameter vesicles, the TF content was varied from 1 to more than 64 TF molecules per vesicle, (ii) keeping one TF molecule per vesicle constant, we examined vesicles with diameters ranging from 10 to 400 nm, and (iii) naked vesicles were added to each preparation. We then determined the K_m and k_{cat} of different preparations using initial velocity techniques, keeping substrate hydrolysis to <10%. Although the term "initial velocity" traditionally implies that no product has been generated and hence no product inhibition can be observed, in reality, when these techniques are used, many product molecules are generated over the short time course of the measurement and if the product is inhibitory, an effect can be, and in fact is, observed.

To investigate the effect of the number of TF molecules per vesicle on K_m and k_{cat}, we prepared PSPC vesicles containing approximately 1, 2, 8, or 64 TF molecules per vesicle and performed initial velocity measurements of F.Xa generation in the presence of varying concentrations of F.X. The K_m and V_{max} of each substrate versus velocity curve was determined from a hyperbolic fit, and the k_{cat} calculated from the expected number of functional TF/VIIa complexes, assuming only half of the TF molecules are facing outward from the vesicle and are hence functional. Three to four substrate−velocity curves were performed for each TF−PSPC preparation and the mean k_{cat} and K_m reported. Interestingly, as the surface density of TF was increased, the apparent k_{cat} decreased from 914 to 469 min (see Figure 6, left). The K_m changes relatively little, increasing from 14 to 22 nM. One possible explanation for a decrease in the catalytic rate constant of TF/VIIa is that the TF or TF/VIIa is self-inhibiting, even though the surface densities of the enzyme studied here are sparse. If there is any finite affinity between the TF molecules (or complexes), then we postulate they may cluster and become less active. An alternative explanation, considered later, is that product inhibition is more potent at high-TF densities because the product influences neighboring TF/VIIa complexes.

To minimize the possibility of TF clustering, we prepared vesicles of different sizes (10, 30, 50, 100, 200, or 400 nm diameter) with only 1 TF per vesicle; hence, the amount of PSPC associated with each TF molecule is controlled by the size of the vesicle instead of the number of TF molecules per vesicle. Four to six substrate−velocity curves were performed on each preparation and the K_m and k_{cat} determined as described above. As the diameter of the vesicle was increased from 10 to 50 nm, the apparent k_{cat} ($k_{cat,app}$) increased dramatically (see Figure 6, right). As the vesicle diameter was further increased to 400 nm, the apparent k_{cat} tended to asymptotically approach a maximum. A hyperbolic fit of the $k_{cat,app}$ values ($r^2_{adj} = 0.94$) indicated a maximum, or true k_{cat}, of 1500/min, and that a 40 nm-diameter vesicle would exhibit a $k_{cat,app}$ that was 50% of the maximum. There was a marginal decrease in the K_m, from 28 to 11 nM, as the vesicle size was increased from 10 to 400 nm. Thus, the amount of lipid associated with TF appears to regulate the apparent catalytic rate constant of the TF/VIIa complex.

Because we varied the size of the vesicles while keeping the TF concentration constant, the PSPC concentration varied

Table 1: A Review of Binding Measurements of F.X and F.Xa to Phospholipid Surfaces

ligand	phospholipid PS/PC ratio	K_D (nM)	maximum binding (pmol/cm^2)	technique	reference
X	25/75	470	NA[a]	light scattering	*1*
X	33/33/33PE	340	NA[a]	light scattering	*23*
X	25/75	40	NA[a]	light scattering	*17*
Xa	25/75	580		light scattering	*17*
X	25% Folch III	2500	NA[a]	light scattering	*20*
Xa	25/75	2700		fluorescence	*19*
X	25/75	39	NA[a]	plasmon resonance	*3*
Xa	25/75	65	NA[a]	plasmon resonance	*3*
Xa	20/80	47		ellipsometry	*13*
Xa	25/75	33	12	flow reactor	*6*
Xa	25/75	114		light scattering	*18*
Xa	30/70	54	8.5	ellipsometry	current data
X	30/70	34	4.2	ellipsometry	current data

[a] NA, not applicable.

with each preparation. To verify that the observed effect was not due to changes in the total lipid concentration, naked 100 nm-diameter vesicles were added to each preparation described above such that the final lipid concentration was 3 μM. Interestingly, in all the paired experiments in which naked vesicles were added, there was a small, but very consistent, 8−20% increase in the apparent k_{cat} (see Figure 6, right); however, this enhancement was small compared to the ~600% increase in signal due to vesicle size. For example, when naked vesicles were added to the 10 nm-diameter vesicle preparation thereby increasing the concentration of PSPC from 0.004 to 3 μM (800-fold), there was only an 8% increase in the apparent k_{cat}. This limited effect on k_{cat} by naked lipid is likely associated with the relief of F.Xa-induced inhibition as the naked lipid provides alternative F.Xa-binding sites away from the enzyme complex. However, the time delay associated with F.Xa leaving the active vesicle surface and reaching quasi-equilibrium on a distant vesicle is likely large thereby explaining the small 8% enhancement. Therefore, the large changes in the apparent k_{cat} described earlier must be associated with the spatial proximity of PSPC to the enzyme.

DISCUSSION

In this study, we show that the phospholipid area surrounding a TF molecule acts as a conduit for substrate presentation and product removal. Under the conditions commonly employed, this surface would be crowded with protein molecules, which, in turn, leads to hindered surface diffusion (*16*). Insofar as surface-movement of FX and FXa controls the reaction rate, conditions that favor relief of crowding could affect the reaction rate. We present evidence showing that the reaction product, F.Xa, competes more effectively for binding to the PSPC membrane than F.X under conditions of limiting phospholipid. The preferential binding of F.Xa coupled with the spatial proximity to the enzyme of F.Xa generated in situ, leads to high local surface densities of F.Xa, which slows the trafficking of F.X and F.Xa on the surface and favors product inhibition.

Although the binding of F.X and F.Xa to PSPC has been studied extensively, the binding parameters describing this interaction vary considerably throughout the literature (see Table 1). Using ellipsometry, we measured the dissociation constants of F.X and F.Xa as 34.2 nM and 53.9 nM, respectively, which agree well with several other recent measurements using a variety of techniques (*3*, *6*, *13*, *17*), but disagree with those of others (*1*, *18*−*20*). Unexpectedly, we found the maximum binding of F.Xa to PSPC at saturation to be twice that of F.X. On the basis of cross sections taken from the structures of F.X and F.Xa (*15*), we calculated the 2D-packing efficiency of a F.Xa monolayer at saturation would be 86%, which would be exceptionally well-organized and much higher than the 2D-packing efficiency for F.X (56%). Moreover, studies by Majumder (*21*) have indicated that F.Xa may dimerize in the presence of PS. This led us to construct a sequential dimer model in which F.Xa first binds to the PSPC surface, and then a second molecule of F.Xa binds from solution to the already bound F.Xa molecule. The ellipsometry binding data for F.Xa were found to fit the dimer model extremely well and suggest that F.X and F.Xa may have approximately equal affinities for PSPC and differ solely by virtue that a second F.Xa can bind as a dimer (K_b = 83 nM). Numerical simulations of the competition of F.X and F.Xa for the membrane using the dimer model indicated that at low phospholipid concentrations the membrane would be almost entirely occupied by F.Xa, whereas a monomer model suggested they would be nearly equal. Experiments of F.X and F.Xa binding with low lipid demonstrated that virtually all of the bound protein was F.Xa, thus indicating the dimer scheme was a better model. Additional simulations with the dimer model indicated that at low lipid concentrations (relative to the quantity of F.X and F.Xa present) F.Xa is preferentially bound to the PSPC surface, thereby diminishing the surface density of substrate (F.X). As the lipid concentration is increased, there is less F.Xa bound per unit area and the surface density of F.X goes through a maximum. At high lipid concentrations, the surface densities of F.X and F.Xa are similar and sparse, and both decrease with added lipid. Thus, if the activity of TF/VIIa is dependent upon the local surface density of F.X, then we would expect that, in accord with our data (Figure 1), there is an intermediate concentration of PSPC that yields optimal F.Xa generation, which is what we observed.

Consistent with the idea that F.Xa binds preferentially at low lipid concentrations, we found that F.Xai was a much stronger inhibitor of TF/VIIa at lower lipid concentrations. The enhanced inhibition can be attributed to the preferential binding of F.Xa to the lipid, which creates high surface densities of F.Xa near the enzyme. These high surface densities can inhibit F.X activation by limiting the amount of F.X that can bind to the surface, by hampering the surface diffusion of F.X on the surface, and by favoring the formation

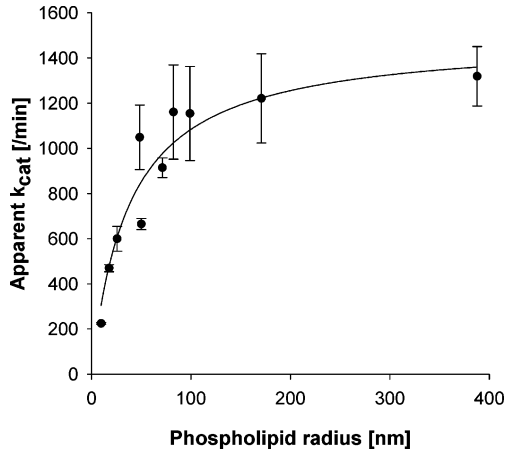

FIGURE 7: The experimentally determined k_{cat} values from experiments in which the number of TF molecules per vesicle was varied and from experiments in which the size of the vesicle was varied while keeping one TF per vesicle are plotted as a function of the 2D radius of phospholipid associated with each functional TF/VIIa complex. The data were fit to a hyperbola indicating that when the lipid radius is large the observed k_{cat} approaches a maximum or "true k_{cat}" of 1500/s. The 2D radius yielding 50% of the maximum rate is 37.7 nm or approximately 8 F.X diameters. Naked lipid vesicles were not considered to be associated with TF and had little effect on the apparent k_{cat}.

of enzyme−inhibitor instead of enzyme−substrate complexes. This type of inhibition suggests it would be relieved by increasing the concentration or surface density of available F.X, a model that predicts only a change in the $K_{m\ app}$. In additional studies, we have found that much of the F.Xai-mediated inhibition is mixed and results from an increase in the apparent K_m as well as a decrease in the $k_{cat\ app}$. Whereas experiments with F.Xai are associated with a random distribution of the inhibitor at the start of the reaction, F.Xa is generated in situ and likely forms a density gradient around each enzyme, thus enhancing the inhibitory potency.

The most pronounced effects of PSPC on TF activity were observed when we regulated the 2D-phospholipid surface area available to each enzyme complex. This was done by either varying the number of TF molecules per 100 nm-diameter vesicle or by varying the size of the vesicle while keeping approximately one TF molecule per vesicle. In both sets of experiments, we consider that each TF molecule was constrained to a functional 2D-phospholipid radius of r_{2D}, where D_v is the diameter of the vesicle and N is the functional number of TF molecules per vesicle. (Basically this is the PSPC surface area associated with each functional TF molecule mapped onto the area of a circle of radius r_{2D}. Naked vesicles were not considered associated with TF.)

$$r_{2D} = \frac{D_v}{\sqrt{N}}$$

When the apparent k_{cat} data from both sets of experiments are presented as a function of the 2D-phospholipid radius, we find that both data sets match and describe the same trend (see Figure 7). A hyperbolic fit of these data indicated the apparent k_{cat} approaches a maximum of 1500/min at very large phospholipid radii, which we believe to be the "true" k_{cat}. The phospholipid radius at which the apparent k_{cat} is half-maximum is 38 nm ($r^2_{adj} = 0.94$). As it is doubtful that lipid more than 40 nm away from the enzyme complex could have a direct, conformational effect on the enzyme complex, the phospholipid effect on $k_{cat\ app}$ is likely due to membrane interactions with F.X and F.Xa. Thus, we propose the reaction is limited by the leaving rate of F.Xa from the lipid about the enzyme complex.

We contend that F.Xa leaves the enzyme complex laterally along the lipid surface, and then leaves the vicinity of the enzyme by either continued lateral diffusion or by desorption from the PSPC surface. Hence, the rate of F.Xa leaving the vicinity of the enzyme may regulate the rate at which F.X enters. Using plasmon resonance, Erb et al. (*3*) have reported an off-rate of F.Xa from PSPC of ~2 per minute, which translates to a half-time of ~17 s, a figure we have confirmed (data not shown). This off-rate is slow compared to k_{cat} (1500/min) and likely results in a local accumulation of F.Xa on the surface near the enzyme, especially under conditions in which the phospholipid radius about the enzyme is constrained. A larger phospholipid radius would allow the F.Xa to diffuse further away from the enzyme, thus increasing the overall rate at which F.Xa leaves the vicinity of the enzyme and minimizing the local accumulation of F.Xa. Findings from the dimer model, that F.Xa competes more effectively for the lipid than F.X, would further elevate the local surface density of F.Xa. Moreover, results from the dimer model were based on equilibrium binding studies where F.X and F.Xa compete for the lipid surface starting from free solution; in the case of F.Xa generated by TF/VIIa on the surface, the F.Xa is ipso facto already bound to the surface.

Increased local densities of F.Xa in a small phospholipid radius near the enzyme could inhibit the reaction in several ways: (i) a surface crowded with F.Xa (or any lipid binding protein), would leave few vacant sites for F.X to bind, (ii) high local concentrations of F.Xa near the enzyme would favor the formation of an enzyme−product complex as opposed to an enzyme−substrate complex, and (iii) high surface densities of any protein on a surface tend to result in decreased lateral diffusion and thus a decreased number of collisions between the lipid-bound substrate and the enzyme. Because additional substrate would not affect the off-rate of Xa from the surface, we reason that the kinetic effect would be manifested as a decrease in the $k_{cat\ app}$, which is in agreement with our findings.

Interestingly, we did observe an enhancement in the reaction rate and in the apparent k_{cat} with the addition of naked vesicles. However, this enhancement was small (8−20%) compared to the 6-fold enhancement observed when TF-associated lipid was added to the same reaction. In one particular experiment, we increased the concentration of lipid 800-fold by adding naked vesicles and observed only an 8% increase in the apparent k_{cat}. We believe the small enhancement observed in the presence of naked vesicles results from the relief of F.Xa-induced inhibition. The additional lipid provides a sink for F.Xa, which alleviates the surface crowding of F.Xa near the enzyme. However, as the added lipid is far from the enzyme (and as we believe the off-rate from PSPC is slow) the overall effect is small. Lipid added directly to the same vesicle as the enzyme appears more efficient at alleviating the F.Xa-induced inhibition.

Our data and formulation are consistent with a model in which the localization of F.X and F.Xa is a dominant determinate of TF activity. We conclude that the application

of methods that utilize averaging techniques (such as concentration or surface density) are limited and of questionable value. We suggest that stochastic, particle-tracking simulations present the best opportunity to understand this important physiological reaction.

APPENDIX A

We developed these equations describing the sequential dimer model for F.Xa binding to lipid, where all species are at equilibrium. Product (P) is the concentration of free F.Xa, L is the nanomoles per liter of lipid binding sites, LP is the nanomoles per liter of lipid-bound F.Xa, and LD is the nanomoles per liter of lipid-bound F.Xa dimer. In this model, one free F.Xa molecule binds to one lipid-binding site, and then a second free F.Xa molecule can bind to the first.

$$P + L \overset{K_a}{\leftrightarrow} \mathrm{LP}$$

$$P + \mathrm{LP} \underset{K_b}{\longleftrightarrow} \mathrm{LD}$$

At equilibrium, the relationship between product, lipid binding sites, and lipid-bound product can be described by the following equations:

$$\mathrm{LP} = L \cdot P / K_a \quad (1)$$

$$\mathrm{LD} = P \cdot \mathrm{LP} / K_b \quad (2)$$

The total concentration of lipid binding sites in the system is L_{tot}.

$$L_{tot} = L + \mathrm{LP} + \mathrm{LD} \quad (3)$$

Solving eqs 1, 2, and 3 for L gives

$$L = L_{tot}/(1 + P/K_a + P^2/K_a/K_b) \quad (4)$$

Similarly, the total concentration of product in the system is P_{tot}.

$$P_{tot} = P + \mathrm{LP} + 2 \cdot \mathrm{LD} \quad (5)$$

Substitute in the values of LP, LD, and L from eqs 1, 2, and 4 into eq 5,

$$P^3 + P^2 \cdot (K_b + 2 \cdot L_{tot} - P_{tot}) + P(K_a \cdot K_b + K_b \cdot L_{tot} - K_b \cdot P_{tot}) - K_a \cdot K_b \cdot P_{tot} = 0 \quad (6)$$

The total lipid concentration (PSPC_{tot}) was measured by ellipsometry, but this does not give the number of lipid binding sites (L_{tot}). The parameter, n, is the ratio of the number of PSPC molecules to protein molecules at saturation. Therefore, in the case of the dimer model, half of those F.Xa molecules are in direct contact with the lipid, and the other half are forming the second half of the dimer. Hence,

$$L_{tot} = \mathrm{PSPC}_{tot}/(2n) \quad (7)$$

Substituting this into eq 6 gives

$$P^3 + P^2[K_b + (\mathrm{PSPC}_{tot}/n) - P_{tot}] + P \cdot [K_a \cdot K_b + (K_b \cdot \mathrm{PSPC}_{tot}/2n) - K_b \cdot P_{tot}] - K_a \cdot K_b \cdot P_{tot} = 0 \quad (8)$$

The concentration of free F.Xa is the one positive real solution to this cubic between 0 and (P_{tot}). Basically, we apply the classic solution where a_3, a_2, a_1, and a_0 are the ordered coefficients of the cubic equation. Let

$$Q = (a_1/3) - (a_2^2/9)$$

$$R = (a_1 a_2 - 3a_0)/6 - a_2^3/27$$

$$S_1 = (R + (Q^3 + R^2)^{1/2})^{1/3}$$

$$S_2 = (R - (Q^3 + R^2)^{1/2})^{1/3}$$

The solution of interest is

$$P = S_1 + S_2 - (a_2/3)$$

and consequently, the bound concentration of F.Xa (P_{bound}) is

$$P_{bound} = P_{tot} - P$$

The values of bound F.Xa measured during ellipsometry (P_{bound}) were fit to the calculated values using the Levenberg−Marquardt method to determine K_a, K_b, and n. In a special case, we assumed K_a and n were identical to those of F.X binding to PSPC and only fit the dimeric dissociation constant, K_b.

APPENDIX B

In this section, we consider the competition of F.X and F.Xa for binding to a phospholipid surface using two separate approaches. In both of these approaches, we consider the particular affinities of F.X and F.Xa for the phospholipid and the maximum number of protein molecules per unit area of phospholipid. In neither case does one molecule displace the other from the surface. In both of these approaches, we identify the time derivatives of each species and calculate the steady-state, equilibrium solution.

Monomeric Binding Model. In the monomeric binding model, F.Xa exists only as a monomer on the lipid surface. F.X and F.Xa compete for lipid surface area with F.Xa requiring half the surface area as F.X; this allows twice as many F.Xa molecules to fit on the surface as F.X molecules. The mechanism underlying this type of competition and the differences in the surface area required by F.X and F.Xa may be related to an unusual geometric orientation of the molecules on the surface, to a difference in the requirement of F.X and F.Xa for PS residues,or something else that has yet to be elucidated. The approach of assigning a surface area to each bound molecule of F.X or F.Xa is general in nature and may account for a variety of mechanisms involving the protein lipid interaction.

From ellipsometry measurements, we know the number of PSPC molecules per unit area in the bilayer and the maximum number of F.X and F.Xa molecules that can bind to each unit of PSPC surface area. From this, we define the PSPC surface area occupied by each unit of

protein (alS,alP) or the area presented by each unit of lipid (alL).

$$\text{alS} = 1/0.004\ 2\ [\text{cm}^2/\text{nmol}] = \text{PSPC surface area occupied per nmole of bound F.X}$$

$$\text{alP} = 1/0.008\ 5\ [\text{cm}^2/\text{nmol}] = \text{PSPC surface area occupied per nmole of bound F.Xa}$$

$$\text{alL} = 1/0.443\ [\text{cm}^2/\text{nmol}] = \text{PSPC surface area presented per nmol of PSPC}$$

The schematic model of (*S*) substrate and (*P*) product binding to available lipid surface area is given below, where k_i (i = 4..7) are the on and off rates as shown. The ratios of k_5/k_4 and k_7/k_6 matched the monomeric dissociation constants fit from ellipsometry and were similar to those reported by Erb using plasmon resonance studies (*3*). Perturbing the k_i values while keeping the ratios k_5/k_4 and k_7/k_6 constant does not affect the steady-state equilibrium solutions.

$$S + L \underset{k_5}{\overset{k_4}{\leftrightarrow}} \text{LS}$$

$$P + L \underset{k_6}{\overset{k_7}{\leftrightarrow}} \text{LP}$$

The mathematical model of this system consisting of the time derivatives of each species is given below, were LP is lipid-bound product, *P* is free product, and *S* is free substrate, all in nmol/L. *L* is the available surface area in cm^2/L.

$$\text{LP}' = (k_6 \cdot P \cdot L/\text{alP}) - (k_7 \cdot \text{LP})$$

$$L' = k_5 \cdot L \cdot S \cdot \text{alS} - k_4 \cdot S \cdot L + k_7 \cdot \text{LP} \cdot \text{alP} - k_6 \cdot P \cdot L$$

$$P' = k_7 \cdot \text{LP} - (k_6 \cdot P \cdot L/\text{alP})$$

$$S' = k_5 \cdot \text{LS} - (k_4 \cdot S \cdot L/\text{alS})$$

$$\text{LS}' = (k_4 \cdot S \cdot L/\text{alS}) - k_5 \cdot \text{LS}$$

The initial values of LP and LS are set to 0, whereas *P* and *S* are set to the total amount of product and substrate we wish to simulate. The initial value of *L* is the product of the amount of PSPC added (or in the bilayer) and alL. The equations were solved using a Fortran implementation of the LSODE solver from Livermore Labs (*22*) and the steady-state equilibrium solution determined from the terminal values after the system reached an apparent steady state.

Dimer Binding Model. In the dimer binding model, both F.X and F.Xa compete for identical PSPC binding sites but have different affinity for these sites. F.Xa can form a dimer on the lipid surface when a free F.Xa binds an already bound F.Xa molecule. The on and off rates are given by k_i (i = 4..7). These are chosen so that their respective ratios are equal to the dissociation constants fit from ellipsometry. Actual rates are similar to those reported by Erb (*3*), and perturbations in these numbers while keeping the dissociation constant ratios constant had no effect on the steady-state solutions.

$$S + L \underset{k_5}{\overset{k_4}{\leftrightarrow}} \text{LS}$$

$$P + L \underset{k_{11}}{\overset{k_{10}}{\leftrightarrow}} \text{LP}$$

$$P + \text{LP} \underset{k_9}{\overset{k_8}{\leftrightarrow}} \text{LD}$$

The time derivative of each species is given below, were LP is lipid-bound product, LD is lipid-bound dimer, *P* is free product, *S* is free substrate, and *L* is the available binding sites, all in units of nmole/L.

$$\text{LP}' = k_{10} \cdot P \cdot L - k_{11} \cdot \text{LP} + k_9 \cdot \text{LD} - k_8 \cdot P \cdot \text{LP}$$

$$\text{LD}' = k_8 \cdot P \cdot \text{LP} - k_9 \cdot \text{LD}$$

$$L' = k_5 \cdot \text{LS} - k_4 \cdot S \cdot L + k_{11} \cdot \text{LP} - k_{10} \cdot P \cdot L$$

$$P' = k_{11} \cdot \text{LP} - k_{10} \cdot P \cdot L + k_9 \cdot \text{LD} - k_8 \cdot P \cdot \text{LP}$$

$$S' = k_5 \cdot \text{LS} - k_4 \cdot S \cdot L$$

$$\text{LS}' = k_4 \cdot S \cdot L - k_5 \cdot \text{LS}$$

The initial values of LP, LD, and LS were set to 0, whereas *P* and *S* were set to the total amount of product and substrate we wished to simulate. The initial value of *L* is the concentration of lipid binding sites calculated as $\text{PSPC}_{\text{tot}}/n$, where *n* was determined from maximal F.X binding. The equations were solved using a Fortran implementation of the LSODE solver from Livermore Labs and the steady-state equilibrium solution determined.

REFERENCES

1. Krishnaswamy, S., Field, K. A., Edgington, T. S., Morrissey, J. H., and Mann, K. G. (1992) Role of the membrane surface in the activation of human coagulation factor X, *J. Biol. Chem. 267*, 26110−26120.
2. Berg, H. C. (1983) *Random Walks in Biology*, Princeton University Press, Princeton, N.J.
3. Erb, E. M., Stenflo, J., and Drakenberg, T. (2002) Interaction of bovine coagulation factor X and its glutamic-acid-containing fragments with phospholipid membranes. A surface plasmon resonance study, *Eur. J. Biochem. 269*, 3041−3046.
4. Bolton, A. E., and Hunter, W. M. (1973) The labelling of proteins to high specific radioactivities by conjugation to a 125I-containing acylating agent, *Biochem. J. 133*, 529−539.
5. Miletich, J. P., Broze, G., J., and Majerus, P. W. (1981) Purification of human coagulation factors II, IX and X using sulfated dextran beads, *Methods Enzymol. 80*, 221−228.
6. Andree, H. A. M., Contino, P. B., Repke, D., Gentry, R., and Nemerson, Y. (1994) Transport rate limited catalysis on macroscopic surfaces: the activation of factor X in a continuous flow enzyme reactor, *Biochemistry 33*, 4368−4374.
7. Bock, P. E. (1992) Active-site-selective labeling of blood coagulation proteinases with fluorescence probes by the use of thioester peptide chloromethyl ketones. II. Properties of thrombin derivatives as reporters of prothrombin fragment 2 binding and specificity of the labeling approach for other proteinases, *J. Biol. Chem. 267*, 14974−14981.
8. Bhairi, S. M. (2001) *Detergents: A Guide to the Properties and Use of Detergents in Biological Systems*, CalBiochem, La Jolla, CA.

9. Cuypers, P. A., Corsel, J. W., Janssen, M. P., Kop, J. M., Hermens, W. T., and Hemker, H. C. (1983) The adsorption of prothrombin to phosphatidylserine multilayers quantitated by ellipsometry, *J. Biol. Chem. 258*, 2426−2431.
10. Andree, H., Hemrmens, W., Hemker, H., and Willems, G. (1992) Displacement of factor Va by annexin V, in *Phospholipid Binding and Anticoagulant Action of Annexin V* (Andree, H., Ed.) pp 73, Universitaire pers Maastricht, Maastricht, The Netherlands.
11. Rand, J. H., Wu, X. X., Andree, H. A., Ross, J. B., Rusinova, E., Gascon-Lema, M. G., Calandri, C., and Harpel, P. C. (1998) Antiphospholipid antibodies accelerate plasma coagulation by inhibiting annexin-V binding to phospholipids: a "lupus procoagulant" phenomenon, *Blood 92*, 1652−1660.
12. Andree, H. A., Stuart, M. C., Hermens, W. T., Reutelingsperger, C. P., Hemker, H. C., Frederik, P. M., and Willems, G. M. (1992) Clustering of lipid-bound annexin V may explain its anticoagulant effect, *J. Biol. Chem. 267*, 17907−17912.
13. Giesen, P. L., Willems, G. M., and Hermens, W. T. (1991) Production of thrombin by the prothrombinase complex is regulated by membrane-mediated transport of prothrombin, *J. Biol. Chem. 266*, 1379−1382.
14. Contino, P. B., Hasselbacher, C. A., Ross, J. B., and Nemerson, Y. (1994) Use of an oriented transmembrane protein to probe the assembly of a supported phospholipid bilayer, *Biophys. J. 67*, 1113−1116.
15. Venkateswarlu, D., Perera, L., Darden, T., and Pedersen, L. G. (2002) Structure and dynamics of zymogen human blood coagulation factor X, *Biophys. J. 82*, 1190−1206.
16. Saxton, M. J. (1987) Lateral diffusion in an archipelago. The effect of mobile obstacles, *Biophys. J. 52*, 989−997.
17. McDonald, J. F., Shah, A. M., Schwalbe, R. A., Kisiel, W., Dahlback, B., and Nelsestuen, G. L. (1997) Comparison of naturally occurring vitamin K-dependent proteins: correlation of amino acid sequences and membrane binding properties suggests a membrane contact site, *Biochemistry 36*, 5120−5127.
18. Krishnaswamy, S., Jones, K. C., and Mann, K. G. (1988) Prothrombinase complex assembly. Kinetic mechanism of enzyme assembly on phospholipid vesicles, *J. Biol. Chem. 263*, 3823−3834.
19. Nesheim, M. E., Kettner, C., Shaw, E., and Mann, K. G. (1981) Cofactor dependence of factor Xa incorporation into the prothrombinase complex, *J. Biol. Chem. 256*, 6537−6540.
20. Bloom, J. W., Nesheim, M. E., and Mann, K. G. (1979) Phospholipid-binding properties of bovine factor V and factor Va, *Biochemistry 18*, 4419−4425.
21. Majumder, R., Wang, J., and Lentz, B. R. (2003) Effects of water soluble phosphotidylserine on bovine factor Xa: functional and structural changes plus dimerization, *Biophys. J. 84*, 1238−1251.
22. Hindmarsh, A. C. (1980) LSODE and LSODI: two initial value ordinary differential equation solvers, *ACM-Signum Newsl. 15*, 10−11.
23. Burri, B. J., Edgington, T. S., and Fair, D. S. (1987) Molecular interactions of the intrinsic activation complex of coagulation: binding of native and activated human factors IX and X to defined phospholipid vesicles, *Biochim. Biophys. Acta 923*, 176−186.

BI050338B